



**NOAA NESDIS
National Geophysical Data Center**

**GOES EPEAD SCIENCE-QUALITY
ELECTRON FLUXES
ALGORITHM THEORETICAL BASIS
DOCUMENT
Version 1.0**

GOES EPEAD Science-Quality Electron Fluxes
Algorithm Theoretical Basis Document

TITLE: GOES EPEAD Science-Quality Electron Fluxes
ALGORITHM THEORETICAL BASIS DOCUMENT VERSION 1.0

AUTHORS:
Juan V. Rodriguez

GOES EPEAD Science-Quality Electron Fluxes
ALGORITHM THEORETICAL BASIS DOCUMENT
VERSION HISTORY SUMMARY

Version Number	Date	Authors	Revision Description	Reason for Revision
1.0	September 10, 2014	Juan V. Rodriguez	Initial release	--

TABLE OF CONTENTS

LIST OF FIGURES	8
LIST OF TABLES	9
LIST OF ACRONYMS	10
ABSTRACT	11
1.0 INTRODUCTION	12
1.1 Purpose of This Document	12
1.2 Who Should Use This Document	12
1.3 Inside Each Section	12
1.4 Related Documents	13
2.0 OBSERVING SYSTEM OVERVIEW	14
2.1 Product Generated	14
2.2 Instrument Characteristics	14
3.0 ALGORITHM DESCRIPTION	15
3.1 Algorithm Overview	15
3.2 Processing Outline	15
3.3 Algorithm Input	15
3.3.1 Primary Data	15
3.3.2 Ancillary Data	15
3.4 Theoretical Description	16
3.4.1 Physics of the Problem	16
3.4.2 Mathematical Description	20
3.5 Algorithm Output	25
4.0 PRODUCT TESTING AND QUALITY METRICS	27
4.1 Development History	27
4.2 Comparisons with Legacy Data Sets	31
4.3 Error Bars / Sensitivity to Input Errors	32
4.3 Quality Control Plots	32
5.0 PRACTICAL CONSIDERATIONS	35
5.1 Numerical Computation Considerations	35
5.2 Programming and Procedural Considerations	35
5.3 Quality Assessment and Diagnostics	35
5.4 Exception Handling	36
5.5 Algorithm Validation	36
5.6 Acknowledgments	36
6.0 ASSUMPTIONS AND LIMITATIONS	37
6.1 Constants to be Re-evaluated	37
6.2 Input and Output File Contents and Formats	38
6.3 Performance	38
6.4 Pre-Planned Product Improvements	38
7.0 REFERENCES	40
APPENDIX A: PRODUCT VERSIONS	41
Version 1.0.0	41

APPENDIX B: LIST OF VARIABLES AND METADATA 42

LIST OF FIGURES

Figure 1. Cross sections of the EPEAD dome instrument. Dome D3 is the central dome. From GOESN-ENG-048D, Figure 6-5.	17
Figure 2. Energy loss curves for electrons, protons and alphas in EPEAD Dome D3. From GOESN-ENG-048D, Figure 6-6. L6 is 0.25 MeV, L7 is 1.77 MeV, L8 is 10.5 MeV, and L9 is 40 MeV.	18
Figure 3. Proton geometrical factors for EPEAD Dome D3, channels E1, E2 and P4. Note that ‘E1 (old cal)’ refers to the E1 channel from GOES-7 and prior, which was equivalent to the current E2 channel. From NXT-CAL-102, Figure 2.2.	19
Figure 4. Spurious (out-of-field) geometrical factors for the Dome D3 channels E1, E2 and P4. From NXT-CAL-102, Table 2.5, and GOESN-ENG-048, Table 6-19.	20
Figure 5. GOES 13 E2 (>2 MeV) electron fluxes, 4-11 March 2012, and corrections for proton contamination during a large SEP event that reached the S3 level on the NOAA solar radiation storm scale. The top panel shows the uncorrected (maroon) fluxes and the magnitude of the correction due to solar proton contamination (purple). The second panel shows the flux in the four proton channels (P3-P6) used to correct the electron fluxes. The third panel shows the fractional size of the contamination correction (purple) relative to the uncorrected E2 fluxes. The fourth panel shows the corrected E2 (maroon) fluxes and the $\pm 1\sigma$ range in the dynamic errors (salmon) and the SWPC >2 MeV flux alert level of $10^3 \text{ cm}^{-2} \text{ s}^{-1} \text{ sr}^{-1}$. A dropout in corrected fluxes indicates that the correction was larger than the uncorrected flux. The bottom panel shows the corrected E2 fluxes with fill values at times when the ‘minus 1 sigma’ criterion is less than zero.	28
Figure 6. GOES 13 E2 (>2 MeV) electron fluxes, 4-11 March 2012. Same as the bottom panel in Figure 5, except that the criterion used is ‘minus 2 sigma.’	29
Figure 7. GOES 13 E1 (>0.8 MeV) electron fluxes, 4-11 March 2012, and corrections for proton contamination during the same event as in Figure 5. The format is the same as Figure 5.	29
Figure 8. GOES-15 EPEAD data from January 2013. Top panel shows the dead-time-corrected E1 and E2 fluxes from EPEAD-B and the calculated contamination corrections. The second and third panel show the contamination-corrected fluxes and data quality flags determined using the ‘minus 2 sigma’ criterion. The fourth and bottom panel show the contamination-corrected fluxes and data quality flags determined using the ‘(correction)/(uncorrected flux) = 0.3’ criterion.	30
Figure 9. GOES-13, January 2013. Multiplicative dead-time correction for the EPEAD-A sensor.	31
Figure 10. GOES-13, July 2013. Multiplicative dead-time correction for the EPEAD-A sensor.	31
Figure 11. QC plot for GOES-13, March 2012.	33
Figure 12. QC plot for GOES-13, July 2013.	34

LIST OF TABLES

Table 1. GOES magnetometer and EPEAD inputs to EPEAD Science-Quality Electron Fluxes algorithm	16
Table 2. Logic and energy ranges for EPEAD Dome D3 channels	18
Table 3. Solar proton contamination correction coefficients $\alpha(m,n)$, where m is the index of the solar proton channel and n is the index of the electron channel. The coefficients for E3 are listed for completeness but are not used in the present science-quality product. ...	22
Table 4. Geometrical or geometry-energy factors used in processing GOES 13-15 EPEAD electron channels and solar proton channels used in the contamination correction.	23
Table 5. Description of EPEAD orientation flag	25
Table 6. Contents of the GOES 13-15 EPEAD science-quality electron fluxes and orientation product files. The fill values are -99999 for the fluxes and errors and -99 for the flags.	26
Table 7. Geometrical factors and energies used by SWPC in the real-time processing of EPS/EPEAD electron fluxes.	37

LIST OF ACRONYMS

ATBD	Algorithm Theoretical Basis Document
BRF	body reference frame (spacecraft coordinates)
En	EPEAD electron channel, n = 1, 2, 3
EPEAD	Energetic Proton Electron and Alpha Detector
EPN	earthward-poleward-normal coordinate system
EPS	Energetic Particle Sensor
eV	electron volt
GOES	Geostationary Operational Environmental Satellite
keV	kilo-electron-volt
MAG	Magnetometer
MAGED	Magnetospheric Electron Detector
MAGPD	Magnetospheric Proton Detector
MeV	mega-electron-volt
NGDC	National Geophysical Data Center
pfu	particle flux unit
Pn	EPEAD proton channel, n = 1-7
SEP	solar energetic particle
SWPC	Space Weather Prediction Center

ABSTRACT

The GOES 13-15 EPEAD electron fluxes are currently produced in real time by SWPC in the form of full-resolution, 1-minute-averaged and 5-minute-averaged fluxes. A background- and solar proton contamination correction is applied to the 5-minute fluxes. The innovations in the science-quality EPEAD electron fluxes produced by NGDC retrospectively (all at the 1-minute level) include: (1) application of the non-paralyzable dead-time correction recommended by the sensor vendor, (2) application of the SWPC-derived contamination correction to the 1-minute dead-time-corrected fluxes, (3) calculation of error bars using standard error propagation methods, (4) flagging and filling of the contamination-corrected fluxes when the correction is greater than 30% of the uncorrected fluxes, and (5) determination of an orientation flag that indicates the direction in which each EPEAD is looking. This science-quality data set is produced in the form of monthly files for each satellite containing the data from both of EPEADs on each satellite.

1.0 INTRODUCTION

1.1 Purpose of This Document

The purpose of this document is to describe the design and development of the algorithm for calculating science-quality GOES 13-15 EPEAD electron fluxes and the associated EPEAD orientation flag. The key challenge was to choose an automatic method for flagging the data. Results of the development are documented in order to justify the algorithm that was selected in the end. Product details are also provided.

1.2 Who Should Use This Document

This document is intended for users of the GOES 13-15 EPEAD Science-Quality Electron Fluxes product so that they can understand the strengths and weaknesses of the product and use it properly.

1.3 Inside Each Section

Section 2.0 OBSERVING SYSTEM OVERVIEW:

Describes the product generated and the measurements that serve as input to the algorithm.

Section 3.0 ALGORITHM DESCRIPTION:

Describes the development, theory and mathematics of the algorithm. Describes the logical flow of the algorithm, including input and output flow.

Section 4.0 PRODUCT TESTING AND QUALITY METRICS:

Describes the data product quality metrics and the testing of the algorithm during development.

Section 5.0 PRACTICAL CONSIDERATIONS:

Discusses issues involving numerical computation, programming and procedures, quality assessment and diagnostics and exception handling.

Section 6.0 ASSUMPTIONS AND LIMITATIONS:

Describes assumptions regarding input data contents and formats; instrument performance and characterization data; and potential future changes and improvements.

Section 7.0 REFERENCES:

Provides all references mentioned in the ATBD, except for GOES reports which are listed in 1.4.

Appendix A PRODUCT VERSIONS:

Lists and describes all product versions to date.

Appendix B LIST OF VARIABLES AND METADATA

Lists all variables and their attributes, as well as global attributes.

1.4 Related Documents

Available at <http://www.ngdc.noaa.gov/stp/satellite/goes/documentation.html>:

GOESN-ENG-048D: EPS/HEPAD calibration and data handbook, GOESN-ENG-048, Rev. D, Assurance Technology Corporation, Carlisle, Mass., May 13, 2011

NXT-CAL-102: Calibration report for the EPS Dome Sensor response to protons, NXT-CAL-102, Panametrics, Inc., Waltham, Mass., May 30, 1995

PANA-GOESP-CR3: GOES D, E, F progress report, Energetic Particle Sensor Dome calibration work, PANA-GOESP-CR3, Panametrics, Inc., Waltham, Mass., August 26, 2010

2.0 OBSERVING SYSTEM OVERVIEW

2.1 Product Generated

This algorithm corrects one-minute EPEAD E1 (>0.8 MeV) and E2 (>2 MeV) fluxes for dead time, galactic cosmic ray (GCR) backgrounds and solar proton contamination. It calculates one-sigma error bars using error propagation, and flags and fills corrected fluxes if the ratio of the correction to the uncorrected electron flux is greater than or equal to an empirical constant. This product is new and of science-quality in that (1) the background and contamination corrections are applied at a 1-minute cadence rather than the 5-minute cadence of the real-time processing, (2) it flags the data when they are not valid electron fluxes and replaces the invalid fluxes with fill values, and (3) the dead-time correction is not applied in the real-time processing. It also calculates a new ‘orientation flag’ for the EPEAD. This flag is included in the electron flux files and is also output in a separate file for use outside of the science-quality electron fluxes.

The background- and contamination-correction algorithm used in SWPC’s processing is used here. Therefore, when the fluxes are valid, they should be similar (when averaged to 5-minute cadence) to the corrected fluxes calculated by SWPC. However, prior to January 30, 2014 (1516 UT for GOES-13, 1823 UT for GOES-15), the contribution of channel P6 to the correction was zero in the GOES-13-15 real-time processing. This situation was like the correction used on the GOES-12 data since the GOES-12 P6 and P7 channels had failed. The GOES-12 rather than the GOES-11 set of coefficients were mistakenly adopted for GOES 13-15. Therefore, there is some level of discrepancy between these reprocessed fluxes and the real-time fluxes prior to January 30, 2014. (The SWPC-produced fluxes, archived and made available to the public by NGDC, include the residuals of the correction even when the results are not valid electron fluxes – i.e., no quality flagging and replacement with fill values. There are no plans to recreate this real-time data set exactly as it should have been processed, with the complete set of correction coefficients but without the quality flagging.)

2.2 Instrument Characteristics

The Energetic Particle Sensor (EPS), first flown in its current design on GOES 8, was renamed the Energetic Proton, Electron and Alpha Detector (EPEAD) for GOES 13-15. On this latest series, EPS refers to the suite of instruments comprising EPEAD, MAGED and MAGPD. There are two EPEADs on each satellite, one looking east and one looking west. Of the three electron channels, E1 and E2 are derived from the D3 Dome detector and E3 is derived from the D4 Dome detector [*Onsager et al.*, 1996; *Sellers and Hanser*, 1996]. The geometrical factors are given in section 6.1. Energy discriminators and coincidence logic are used to distinguish electrons and protons of different energies.

3.0 ALGORITHM DESCRIPTION

3.1 Algorithm Overview

This algorithm uses the same background-removal and solar-proton correction as used in SWPC's real-time processing. This correction is a weighted sum of four proton channels from the EPEAD. Data are flagged based on the ratio of the correction to the uncorrected fluxes.

3.2 Processing Outline

Currently, this data set is produced retrospectively at NGDC, augmented every 24 hours. For data from a given month-satellite combination:

- a. Calculate the orientation flag from the 1-min MAG magnetic fields
- b. Correct the EPEAD electron fluxes for dead time
- c. Calculate the proton corrections from EPEAD P3-P6
- d. Subtract the corrections from the uncorrected fluxes
- e. Calculate the error propagation for the corrected fluxes
- f. If the correction is greater than some fraction of the uncorrected fluxes, replace with a fill value and set data quality flag (dqf).
- g. Write one-month science-quality EPEAD electron and orientation flag files.

3.3 Algorithm Input

The inputs to the algorithm consist of 1-minute EPEAD electron and proton uncorrected fluxes and 1-minute MAG magnetic fields in the instrument and spacecraft body reference frames.

3.3.1 Primary Data

The input variables, which are defined in Table 1, are read from the magnetometer and EPEAD electron and proton 1-minute-cadence monthly netCDF files produced routinely by NGDC (see section 6.2).

3.3.2 Ancillary Data

No ancillary data are required by the algorithm.

Table 1. GOES magnetometer and EPEAD inputs to EPEAD Science-Quality Electron Fluxes algorithm

Variables	Refresh	Number of values	Units
time_tag	1 min	1 (start of period)	milliseconds since 1970-01-01 00:00:00.0 UTC
BXSC_1, BYSC_1	1 min	2 (1 per axis)	nT
HN_1, HP_1	1 min	2 (1 per axis)	nT
E1E_UNCOR_FLUX, E2E_UNCOR_FLUX	1 min	2 (1 per channel)	1/(cm ² sr s)
E1W_UNCOR_FLUX, E2W_UNCOR_FLUX	1 min	2 (1 per channel)	1/(cm ² sr s)
P3E_UNCOR_FLUX, P4E_UNCOR_FLUX, P5E_UNCOR_FLUX, P6E_UNCOR_FLUX	1 min	4 (1 per channel)	1/(cm ² sr s MeV)
P3W_UNCOR_FLUX, P4W_UNCOR_FLUX, P5W_UNCOR_FLUX, P6W_UNCOR_FLUX	1 min	4 (1 per channel)	1/(cm ² sr s MeV)

3.4 Theoretical Description

3.4.1 Physics of the Problem

Spacecraft anomalies are known to be caused by electrostatic discharges resulting from the accumulation of charge from penetrating highly relativistic MeV electrons [Garrett and Whittlesey, 2011]. The phenomenon is known as ‘deep charging’ or ‘interior charging.’ The >2 MeV electron channel (E2) is the most heavily used GOES electron channel. In its current form, it first launched on GOES-8 (1994), though an earlier version flew on GOES 4-7. It is used as the basis for a real-time radiation belt alert by SWPC. Because of its importance and its long history, it has been used in much scientific and applied research [e.g., Fennell *et al.*, 2000; Onsager *et al.*, 2004; O’Brien, 2009; Bodeau, 2010; Gannon *et al.*, 2012]. Owing to some historical uncertainty about its characteristics (see section 6.1), the E1 channel has been studied less frequently [e.g., Kress *et al.*, 2014] but has certain advantages over the E2 channel.

The driver for quality flagging of the EPEAD electron channel data is the significant level of proton contamination observed in the E2 channel. This contamination is an unavoidable consequence of the simple instrument design, which attempts to discriminate

species based entirely on energy deposition. The electron channels E1 and E2 are measured by EPEAD Dome D3 (Figure 1), along with proton channel P4 and alpha channel A4. The field-of-view is determined by tungsten collimators that present at least 20 g/cm^2 of shielding to out-of-field particles. The aluminum moderator is 18-mil thick. A 0.145-mil aluminum foil light shield sits atop a pair of 1500 micron, 5.6 mm diameter detectors separated by 5.6 mm that are connected in parallel as a single detector. The four channels are distinguished using logical combinations of four energy thresholds (Figure 2, Table 2).

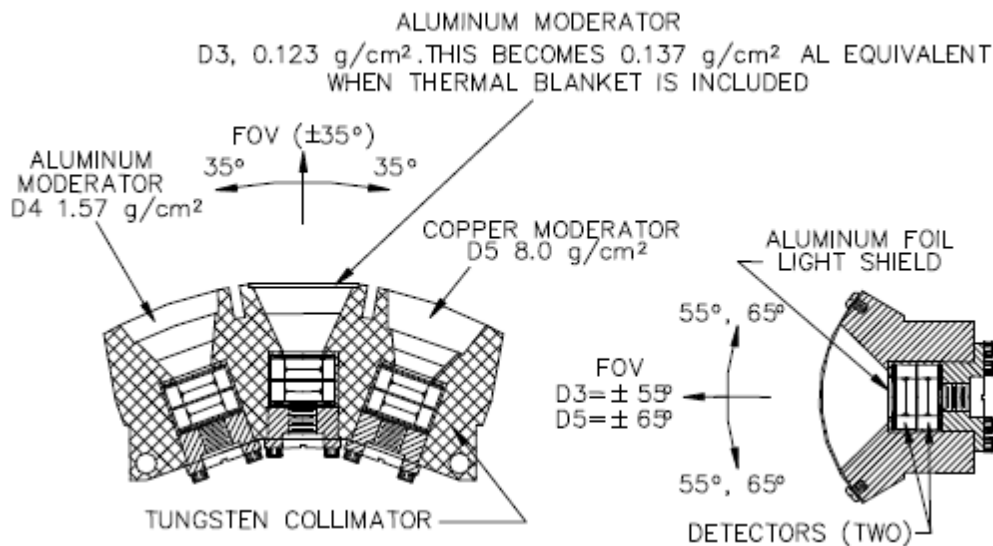


Figure 1. Cross sections of the EPEAD dome instrument. Dome D3 is the central dome. From GOESN-ENG-048D, Figure 6-5.

following description of the multi-branch energy deposition curves follows *Sellers and Hanser* [1996]. The '45 deg' and '0, 60 deg' curves are based on solely on stopping power, neglecting scattering. The maximum path length through the two detectors, at which the particle just penetrates the second detector, is at 45 degrees. The path length at 60 deg, at which the particle only penetrates the first detector, is the same as the minimum path length at 0 deg that penetrates both detectors. The 'total energy loss' curve for electrons assumes that all the kinetic energy remaining after the electron passes through the moderator is deposited in the silicon detectors due to multiple scattering.

The energy loss curves (Figure 2) show that protons below 15 MeV and above 36 MeV (incident energy) deposit energy in the E2 energy loss range. The measured proton geometrical factors for E1, E2 and P4 are shown in Figure 3. They were calculated at 17, 30 and 51 MeV. The normal-incidence effective area measurements spanned a wider energy range, from 13 to 66 MeV [NXT-CAL-102, Table 2.2]. (The geometrical factor is the integral of the effective areas over angle, assuming isotropic flux.) These measurements show that E1 has a measurable response to protons that cannot be inferred from Figure 2, but the E2 response is much larger. Results from the pre-GOES-7

calibrations show that the geometrical factor of the channel equivalent to the current E2 channel is flat from 51 to 66 MeV [PANA-GOESP-CR3, Figure 2.4]. The increase of the geometrical factor with energy can be attributed to the increase in the range of incident angles at which the energy deposited lies below the L8 threshold.

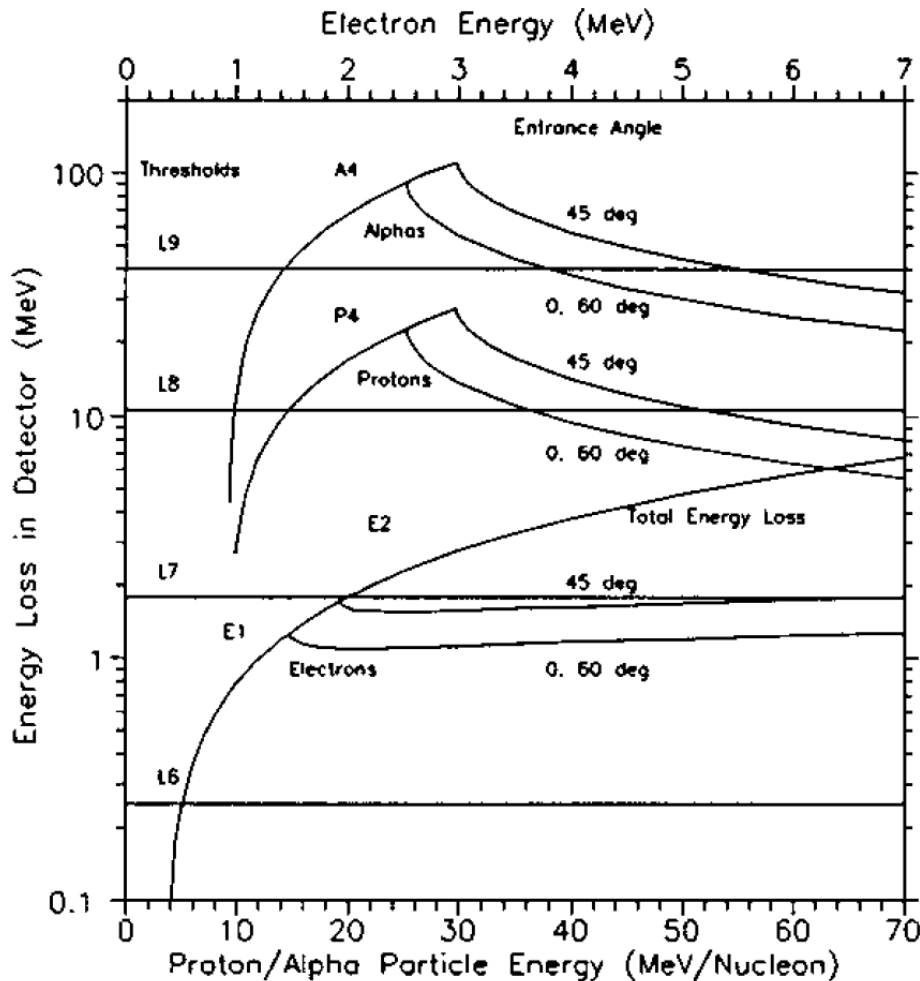


Figure 2. Energy loss curves for electrons, protons and alphas in EPEAD Dome D3. From GOESN-ENG-048D, Figure 6-6. L6 is 0.25 MeV, L7 is 1.77 MeV, L8 is 10.5 MeV, and L9 is 40 MeV.

Table 2. Logic and energy ranges for EPEAD Dome D3 channels

Channel	Particle Type	Coincidence Logic	Incident Energy Range (MeV)	Energy Loss Range (MeV)
E1	Electron	6 • not(7)	>0.6	0.25-1.77
E2	Electron	6 • 7 • not(8)	>2	1.77-10.5
P4	Proton	6 • 8 • not(9)	15-40	10.5-40
A4	Alpha	9	60-160	>40

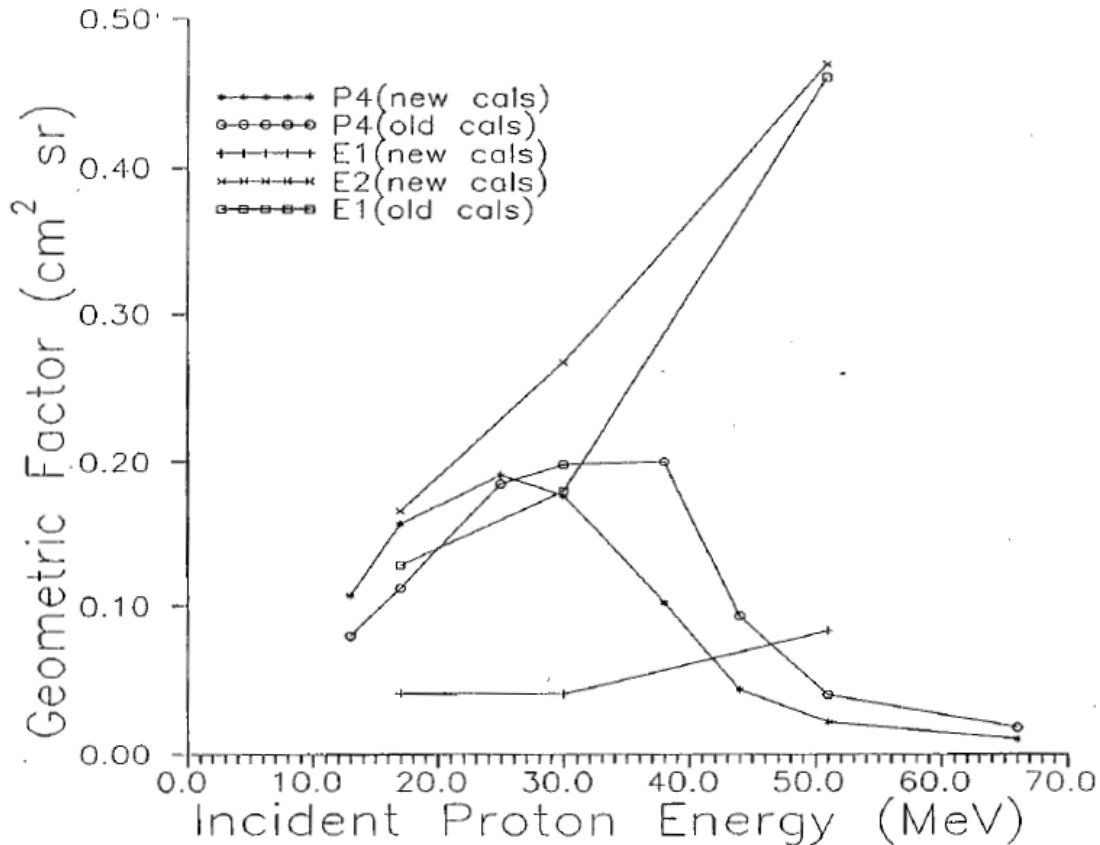


Figure 3. Proton geometrical factors for EPEAD Dome D3, channels E1, E2 and P4. Note that 'E1 (old calcs)' refers to the E1 channel from GOES-7 and prior, which was equivalent to the current E2 channel. From NXT-CAL-102, Figure 2.2.

The foregoing discussion has to do with in-aperture, not out-of-aperture responses. The out-of-aperture (a.k.a 'spurious') proton responses are plotted in Figure 4. They are attributed to rear entry through the copper plug immediately behind the detectors (~80 MeV incident energy threshold) and through the tungsten collimator (~120 MeV threshold) [PANA-GOESP-CR3, p. 28]. Above 90 MeV they are comparable to or larger than the in-aperture responses at lower energies. This characterization is coarse as well as incomplete since the GCR spectrum is fairly flat or increasing from 100 to 1000 MeV, depending on the phase of the solar cycle, and rolls off slowly above that energy [Matthiä *et al.*, 2013].

While these results show that both the E1 and E2 channels are sensitive to protons, the E1 electron geometrical factor is a factor of 15 greater than that of the E2 channel (Table 4), and the incident E1 fluxes are 1-2 orders of magnitude greater than the E2 fluxes. The result is that at geostationary orbit, GCR backgrounds and solar proton events have a negligible effect on the E1 channel, while the E2 channel is dominated by GCR

backgrounds at low count rates (~ 1 c/s) and by solar proton events under most conditions. It is easier therefore to use E2 as a >2 MeV electron flux measurement with confidence if such contamination episodes are removed from the data set.

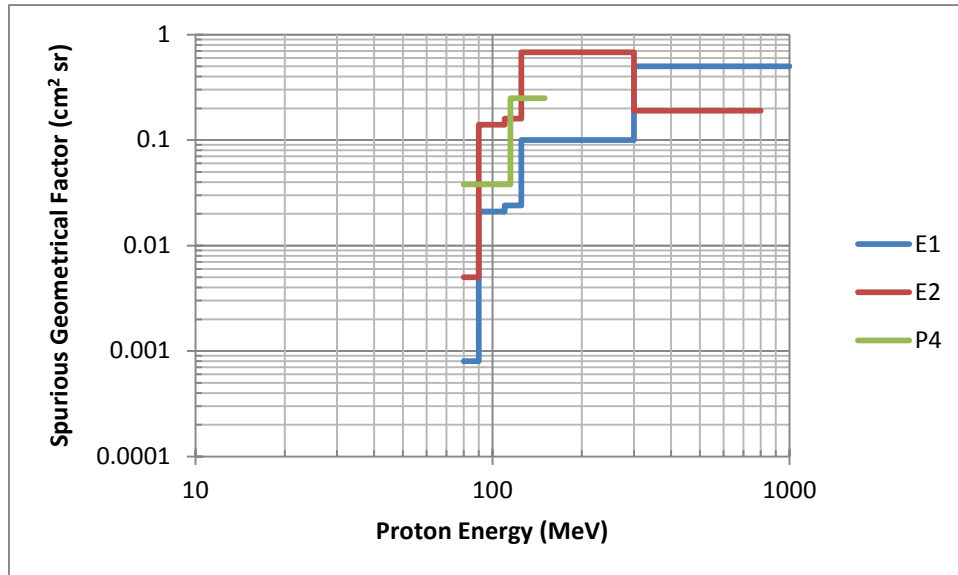


Figure 4. Spurious (out-of-field) geometrical factors for the Dome D3 channels E1, E2 and P4. From NXT-CAL-102, Table 2.5, and GOESN-ENG-048, Table 6-19.

3.4.2 Mathematical Description

Definition of Quantities

$\alpha(m,n)$	coefficient for the contamination contribution of proton channel m to electron channel n ; see Table 3
B_x, B_y, B_z	components of the magnetic field (flux density) vector in spacecraft body reference frame (BRF) coordinates
B_e, B_p, B_n	components of the magnetic field (flux density) vector in the EPN coordinate system
$C_{cc}(n)$	contamination correction to electron channel n in terms of counts
$C_{cor}(n)$	contamination-corrected counts in electron channel n
$C_{dt}(n)$	dead-time corrected but contamination-uncorrected counts in electron channel n
$C_0(n)$	uncorrected counts in electron channel n
Δt	averaging period
η	multiplicative dead-time correction

$G(n)$	geometrical factor for electron channel n , $\text{cm}^2 \text{ sr}$
$j_p(m)$	dead-time corrected but contamination-uncorrected proton differential flux in channel m .
$J(n)$	corrected electron integral flux in channel n
m	proton channel number, $n = 3-6$
n	electron channel number, $n = 1-2$
$R(m \text{ or } n)$	count rate in channel m or n
R_{COR}	contamination-corrected count rate
σ_α	standard deviation in correction coefficients, $\text{cm}^2 \text{ sr MeV}$
σ_G	standard deviation in electron channel geometrical factor, $\text{cm}^2 \text{ sr}$
σ_J	standard deviation in corrected electron integral fluxes
σ_{j_p}	standard deviation in proton differential channel fluxes
σ_R	standard deviation in corrected electron rates
τ	dead time

Dead-time Correction Algorithm

Each EPEAD consists of one telescope and three dome detectors. Each of these four subsystems has its own analog signal processing chain and therefore its own dead time correction. The D3 dome reports four channels: two electron (E1, E2), one proton (P4) and one alpha (A4). The non-paralyzable multiplicative dead-time correction for the D3 dome channels is given by [GOESN-ENG-048D, equation 6.44]:

$$\eta = \frac{1.0}{1.0 - \tau[R(E1) + R(E2) + R(P4) + R(A4)]} \quad (1)$$

where τ is the EPEAD dead time (2.5×10^{-6} s) and $R(\text{channel})$ is the rate in a given channel. The uncorrected fluxes are multiplied by this factor, which is always greater than 1.0. In the current algorithm, this correction is derived from and applied to the one-minute averages.

The dead-time correction is performed before the contamination correction.

Contamination Correction Algorithm

The contamination correction algorithm was derived by H. H. Sauer of the NOAA Space Environment Center in 1995 from the EPS geometrical factors measured by the sensor contractor. It serves double duty in the removal of GCR backgrounds and in the

correction for solar proton fluxes. It uses the uncorrected 1-minute solar proton fluxes from EPS/EPEAD channels P3 (8.7-14.5 MeV), P4 (15-40 MeV), P5 (38-82 MeV), and P6 (84-200 MeV) to correct the 1-minute averages of the EPS/EPEAD electron channels E1 (>0.8 MeV) and E2 (>2 MeV). (Note that the E1, E2 and P4 fluxes have been corrected for the dead time of the D3 dome.) The contamination-corrected count rates R_{COR} are given by

$$R_{COR}(n) = \frac{C_{COR}(n)}{\Delta t} = \frac{C_{dt}(n)}{\Delta t} - \frac{C_{CC}(n)}{\Delta t} \quad (2)$$

where $C_{dt}(n)$ represents the dead-time corrected counts in electron channel n and Δt is the accumulation or averaging period. (The counts, C , are the product of the rates, R , and the accumulation or averaging period, Δt .) The corrected electron integral fluxes are then calculated as:

$$J(n) = \frac{R_{COR}(n)}{G(n)} \quad (3)$$

The contamination correction to the count rates is given by:

$$\frac{C_{CC}(n)}{\Delta t} = \sum_{m=3}^6 \alpha(m, n) j_p(m) \quad (4)$$

where m is solar proton channel 3-6, n is electron channel 1 or 2, Δt is the accumulation or averaging period, and $j_p(m)$ is the uncorrected proton differential flux in channel m . The correction coefficients $\alpha(m, n)$ are given in Table 3 and the geometrical factors are given in Table 4. The latter factors are used to convert from uncorrected fluxes back to rates and counts for the purpose of this algorithm.

Table 3. Solar proton contamination correction coefficients $\alpha(m, n)$, where m is the index of the solar proton channel and n is the index of the electron channel. The coefficients for E3 are listed for completeness but are not used in the present science-quality product.

$\alpha(m, n)$ [cm ² sr MeV]	E1	E2	E3
P3	0.07	0.3	0.0
P4	1.4	9.0	0.9
P5	3.9	18.0	7.6
P6	30.0	96.0	54.0

Table 4. Geometrical or geometry-energy factors used in processing GOES 13-15 EPEAD electron channels and solar proton channels used in the contamination correction.

Channel	G or GdE
E1	0.75 cm ² sr
E2	0.05 cm ² sr
P3	0.325 cm ² sr MeV
P4	4.64 cm ² sr MeV
P5	15.5 cm ² sr MeV
P6	90.0 cm ² sr MeV

The variances in the proton differential fluxes (for proton channels $m = 3$ to 6) are given by:

$$\sigma_{jp}^2(m) = j_p^2(m) \left(\frac{1}{C(m)} + \frac{\sigma_G^2(m)}{G^2(m)} \right) \quad (5)$$

where $C(m)$ are the counts in proton channel m , $G(m)$ is the geometrical factor for proton channel m (Table 4), and $\sigma_G(m)$ is the 1-sigma uncertainty in that geometrical factor.

The variances in the corrected electron rates are given by:

$$\sigma_R^2(n) = \frac{C_0(n)}{(\Delta t)^2} + \sum_{m=3}^6 [\alpha^2(m,n)\sigma_{jp}^2(m) + j_p^2(m)\sigma_\alpha^2(m,n)] \quad (6)$$

where $C_0(n)$ represents the uncorrected counts in electron channel n , Δt is the accumulation or averaging time, $\alpha(m,n)$ are the correction coefficients, and $\sigma_\alpha(m,n)$ are their 1-sigma uncertainties. The relative variance in the corrected electron integral flux is therefore:

$$\frac{\sigma_J^2(n)}{J^2(n)} = \frac{\sigma_R^2(n)}{G^2(n)J^2(n)} + \frac{\sigma_G^2(n)}{G^2(n)} \quad (7)$$

where $J(n)$ is the corrected electron integral flux in channel n , $G(n)$ is the geometrical factor for electron channel n (Table 2), and $\sigma_G(n)$ is the 1-sigma uncertainty in that geometrical factor. The normalized standard deviations in G for both electrons (n) and protons (m), σ_G/G , and in $\alpha(m,n)$, $\sigma_\alpha(m,n)/\alpha(m,n)$, are taken to be 0.25 (25%), although the effective error is larger due to spectral variability.

The positive square root of the quantity in the above equation is reported in the data product as the fractional standard deviation of the corrected fluxes. The absolute error in flux units,

$$\sigma_J(n) = J(n) \sqrt{\frac{\sigma_R^2(n)}{G^2(n)J^2(n)} + \frac{\sigma_G^2(n)}{G^2(n)}} \quad (8)$$

was originally considered as the basis for the automatic quality flagging. As shown in section 4, this quantity becomes comparable to the corrected fluxes when the solar proton flux is significant, and a ‘minus 2 sigma’ criterion for quality flagging was tried:

$$J(n) - 2\sigma_J(n) < 0 \quad (9)$$

This criterion is still available as an option in the software that can be chosen using an IDL keyword. However, it resulted in some “false negatives” under some important circumstances (section 4). Therefore, a simpler criterion was developed: if the ratio of the correction to the uncorrected fluxes exceeds the constant ‘max_corr_ratio’ (currently 0.3), then the corrected fluxes are flagged as invalid (see below) and replaced with fill values. The setting of this constant is by trial-and-error, balancing between rejecting too much (in the extreme, ‘max_corr_ratio’ = 0.0) and too little data (in the extreme, ‘max_corr_ratio’ = 1.0, or greater during large SEP events). We have chosen to err on the side of rejecting some valid fluxes, which is appropriate for a data set from which years of data are commonly analyzed. Researchers interested in the detailed time-series of individual cases should also evaluate the dead-time-corrected fluxes, which are available in the same files.

A data quality flag is determined for each electron channel that pertains to solar proton contamination. It is set to 0 if contamination is sufficiently small that the correction and electron fluxes are valid, i.e., if the ratio of the contamination correction to the uncorrected fluxes is less than the constant ‘max_corr_ratio’. It is set to 1 if contamination is too large and the electron fluxes are not valid, i.e. if the ratio of the correction to the uncorrected fluxes exceeds the constant ‘max_corr_ratio’. It is filled with -99 if there are no data.

Orientation Flag Algorithm

The yaw-flip flag in the SEM housekeeping has a 5-min cadence and does not indicate when a yaw flip is taking place. We have therefore developed a 1-min orientation flag using the 1-min magnetometer field components, thereby benefiting from the work that went into developing that product. During a yaw flip, the spacecraft rotates about the z-axis (pointing toward the earth). This rotates the spacecraft x- and y-axes 180 degrees relative to a coordinate system fixed relative to the orbit plane (the EPN coordinate system). Therefore, whereas when the spacecraft is upright

$$B_p = B_y \quad (10)$$

$$B_n = -B_x \quad (11)$$

the opposite relations hold when the spacecraft is inverted:

$$B_p = -B_y \quad (12)$$

$$B_n = B_x \quad (13)$$

Therefore, the following condition can be used to identify the yaw flip status:

$$k = -\text{round}\left(\frac{B_x}{B_n}\right) + \text{round}\left(\frac{B_y}{B_p}\right) \quad (14)$$

If $k = 2$, then the spacecraft is upright; if $k = -2$, the spacecraft is inverted.

Because GOES 13-15 only provides a two-valued yaw-flip flag, the flag changes state at some point during the yaw-flip maneuver. During the yaw flip, the B_p component exhibits an artificial monopolar dip in its magnitude that is not flagged (at its minimum it represents the in-orbit component of the field). In order to identify when the yaw flip is in progress, we fit a Gaussian function to 61 minutes of the B_p time series centered at the point where the intermediate version of the 1-min flag changes value. Because there is a data outage during the maneuver, there are fill values which must be excluded from this fit. The centroid of this fit is taken to be the midpoint of the flip. The yaw flip period is then identified as a 33 minute period centered at this midpoint. This is based on a nominal 30 minute duration (from observations) plus some margin.

The orientation flag is described in Table 5. It is filled with -99 if there are no data.

Table 5. Description of EPEAD orientation flag

Flag Value	Spacecraft Status	EPEAD-A Orientation	EPEAD-B Orientation
0	upright	eastward	westward
1	inverted	westward	eastward
2	yaw flip in progress	rotating	rotating

3.5 Algorithm Output

The output variables of the GOES 13-15 EPEAD science-quality electron fluxes algorithm are listed in Table 6. They are written into netCDF and csv files (see section 6.2). The orientation flag is written both in the EPEAD electron files and in its own file for ease of use with other EPEAD files (e.g., solar protons and alphas, for which the look direction is much more important [Rodriguez *et al.*, 2010]).

Table 6. Contents of the GOES 13-15 EPEAD science-quality electron fluxes and orientation product files. The fill values are -99999 for the fluxes and errors and -99 for the flags.

Data Type	Refresh	Number of values	Units
time_tag	1 min	1 (start of period)	milliseconds since 1970-01-01 00:00:00.0 UTC
E1E_DTC_FLUX, E2E_DTC_FLUX	1 min	2 (1 per channel)	1/(cm ² sr s)
E1W_DTC_FLUX, E2W_DTC_FLUX	1 min	2 (1 per channel)	1/(cm ² sr s)
E1E_COR_FLUX, E2E_COR_FLUX	1 min	2 (1 per channel)	1/(cm ² sr s)
E1W_COR_FLUX, E2W_COR_FLUX	1 min	2 (1 per channel)	1/(cm ² sr s)
E1E_COR_ERR, E2E_COR_ERR	1 min	2 (1 per channel)	Fractional
E1W_COR_ERR, E2W_COR_ERR	1 min	2 (1 per channel)	Fractional
E1E_DQF, E2E_DQF	1 min	2 (1 per channel)	0 (OK) or 1 (excessively contaminated)
E1W_DQF, E2W_DQF	1 min	2 (1 per channel)	0 (OK) or 1 (excessively contaminated)
ORIENTATION_FLAG	1 min	1	0, 1, 2 (see Table 5)

4.0 PRODUCT TESTING AND QUALITY METRICS

There are two objectives to testing the performance of the EPEAD science-quality electron fluxes processing algorithm. The first objective is to ensure that there are no flaws in the method or implementation of the algorithms. This objective is met by simply comparing the output to that from the legacy processing. The second objective is to provide users with an assessment of the accuracy of the output data. Several accuracy indicators should be considered when using the data. Uncertainty values estimated from Poisson counting statistics are provided with all physical quantities.

Other factors not considered here that may significantly affect performance include response differences between flight models and sensor degradation. These additional factors are discussed further in section 6.1, but accounting for these issues is beyond the scope of the current processing. Users should consider how these limitations in the data accuracy might impact their use or interpretation of the data.

4.1 Development History

In the development of this algorithm, the key challenge was to choose an automatic method for flagging the data. The original approach was to use a criterion based on the standard deviation of the product. While this worked for SEP events, it did not work for GCR backgrounds. Therefore, a criterion based on the magnitude of the contamination correction was developed that worked both for backgrounds and for solar proton contamination.

The first criterion was that the corrected flux would be flagged and replaced with a fill value if the mean minus the standard deviation (equation 8) was less than zero. We found that this was not sufficient to filter out contaminated >2 MeV fluxes at and following the peaks of SEP events, as for example on March 8, 2012 (Figure 5). By a 'minus 2 sigma' criterion (equation 9) was strong enough to filter out these contaminated data without also filtering out valid >2 MeV electron increases in the presence of lower levels of contamination (Figure 6).

For reference the 'minus 2 sigma' results for E1 during this event are shown in Figure 7. The magnitude of the correction to E1 is less than 10%. During a larger SEP event, we can expect the correction to E1 to be larger, particularly during an electron flux dropout, but this figure shows the general insensitivity of E1 to solar proton contamination.

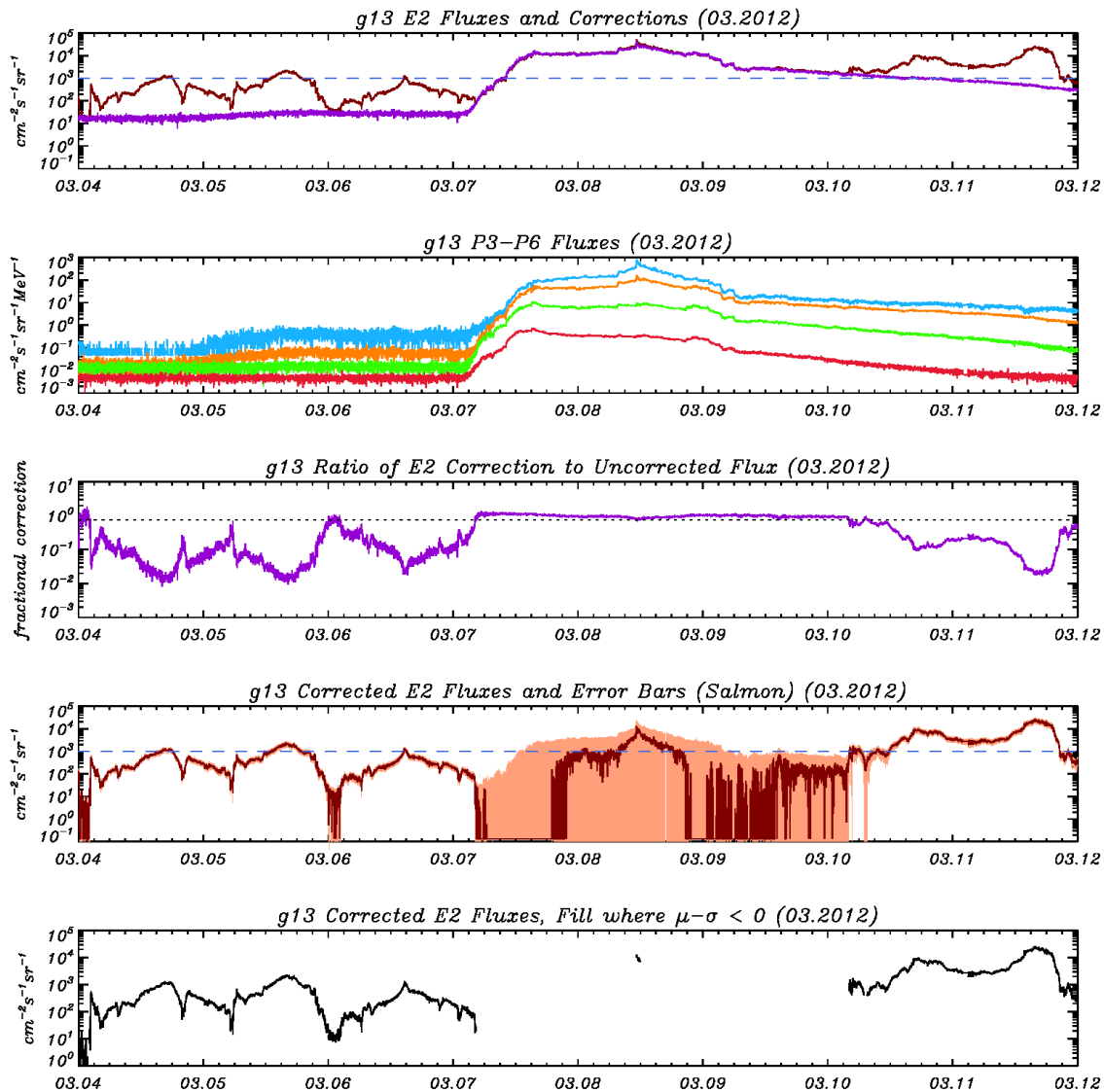


Figure 5. GOES 13 E2 (> 2 MeV) electron fluxes, 4-11 March 2012, and corrections for proton contamination during a large SEP event that reached the S3 level on the NOAA solar radiation storm scale. The top panel shows the uncorrected (maroon) fluxes and the magnitude of the correction due to solar proton contamination (purple). The second panel shows the flux in the four proton channels (P3-P6) used to correct the electron fluxes. The third panel shows the fractional size of the contamination correction (purple) relative to the uncorrected E2 fluxes. The fourth panel shows the corrected E2 (maroon) fluxes and the $\pm 1\sigma$ range in the dynamic errors (salmon) and the SWPC >2 MeV flux alert level of $10^3 \text{ cm}^{-2} \text{ s}^{-1} \text{ sr}^{-1}$. A dropout in corrected fluxes indicates that the correction was larger than the uncorrected flux. The bottom panel shows the corrected E2 fluxes with fill values at times when the 'minus 1 sigma' criterion is less than zero.

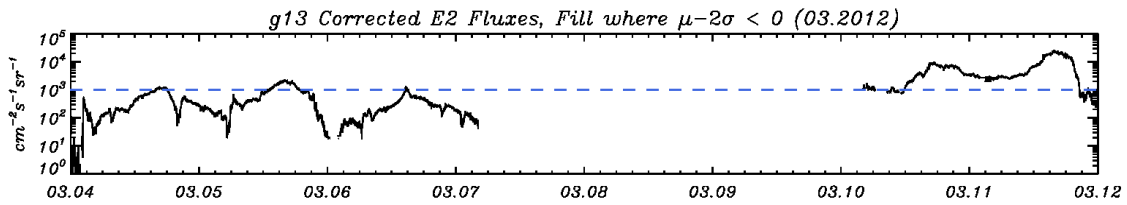


Figure 6. GOES 13 E2 (>2 MeV) electron fluxes, 4-11 March 2012. Same as the bottom panel in Figure 5, except that the criterion used is ‘minus 2 sigma.’

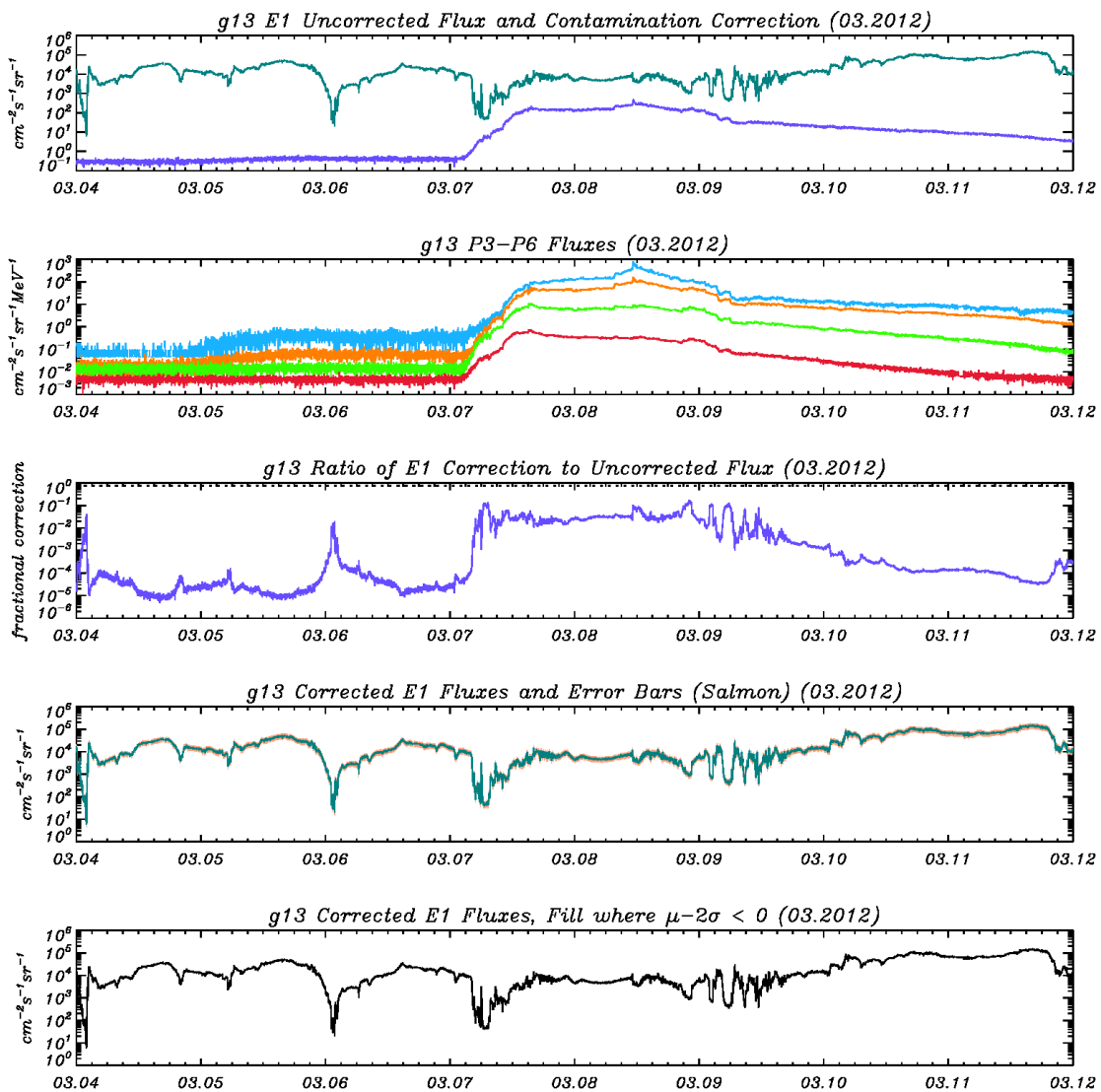


Figure 7. GOES 13 E1 (>0.8 MeV) electron fluxes, 4-11 March 2012, and corrections for proton contamination during the same event as in Figure 5. The format is the same as Figure 5.

The ‘minus 2 sigma’ criterion was not designed to handle background fluxes, however. Because of statistical fluctuations, some backgrounds were still being flagged as valid. An additional, more subtle problem appeared in the course of developing a higher-level product that indicated that the accuracy of the contamination-corrected fluxes near background levels was worse than expected. Between 1 and 13 January 2013, the E2 fluxes hovered around the background level while the E1 fluxes were steadily decreasing overall (Figure 8, panel 1). A temperature estimated from these two spectral points [Gannon *et al.*, 2012] would be steadily increasing at a time when the >0.8 MeV fluxes are decreasing, which is not a physically realistic situation.

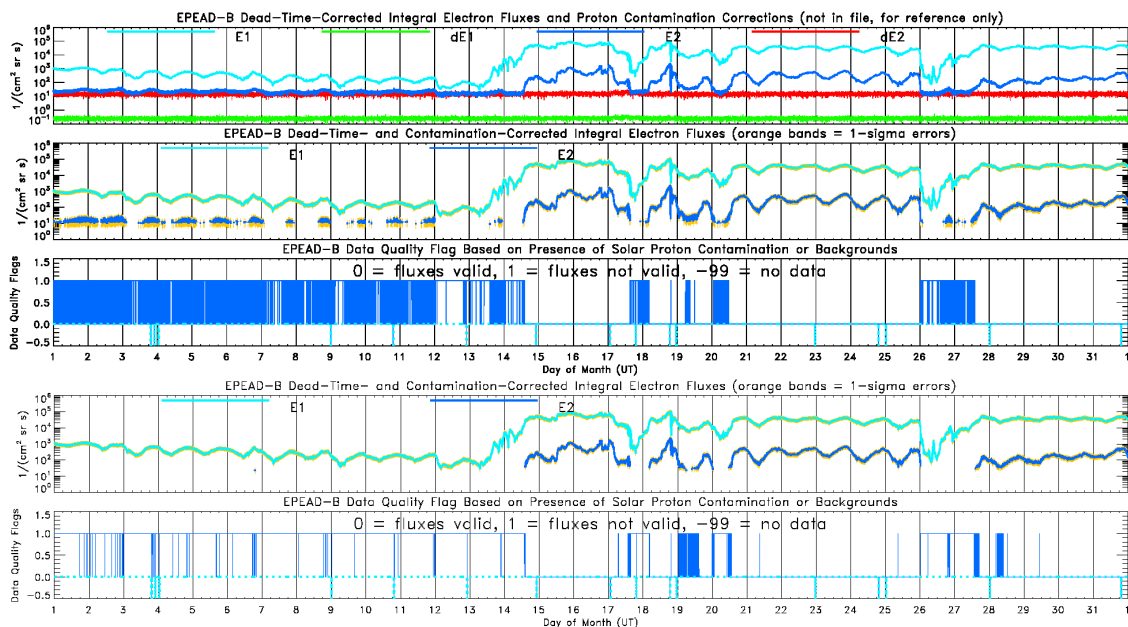


Figure 8. GOES-15 EPEAD data from January 2013. Top panel shows the dead-time-corrected E1 and E2 fluxes from EPEAD-B and the calculated contamination corrections. The second and third panel show the contamination-corrected fluxes and data quality flags determined using the ‘minus 2 sigma’ criterion. The fourth and bottom panel show the contamination-corrected fluxes and data quality flags determined using the ‘(correction)/(uncorrected flux) = 0.3’ criterion.

In order to address this problem, we investigated a criterion based on the magnitude of the contamination correction. We found that it worked much better in flagging background values. Comparison of the 3rd and 5th panels in Figure 8 indicates that the appearance of ‘good’ fluxes amid the invalid fluxes between during 1-13 January 2013 is greatly reduced with this newer criterion. (The dqfs are a more reliable indicator on these plots of the presence of valid fluxes.) Still, routines ingesting these data may wish to use an additional criterion (such as fluxes greater than $30 \text{ 1/(cm}^2 \text{ s sr)}$) for identifying valid fluxes under such conditions. It also worked in the case of SEP-contaminated values. For example, it handled the SEP peak on 8 March 2012 (Figure 11) as effectively as the ‘minus 2 sigma’ criterion.

The original plan was to flag invalid fluxes but keep the as-calculated ‘corrected’ values. However, we received the valid feedback that many users will not read a data quality flag in addition to flux values, despite instructions to the contrary. Therefore, we decided to replace the flagged data with fill values. At this time, the dqf can be used to distinguish whether a fill value is due to excessive contamination or simply due to missing data (because in the latter case the dqf will itself be a fill value).

4.2 Comparisons with Legacy Data Sets

Since there is no duplication of variables between this product and the product coming out of SWPC, no direct legacy comparison is possible. However, a comparison of the uncorrected fluxes from SWPC and the dead-time-corrected fluxes from the present data set is instructive. The ratio of the dead-time-corrected fluxes to the uncorrected fluxes gives the multiplicative dead-time correction (equation 1), apart from those times when one flux is valid and another is invalid, giving an invalid dead-time correction and therefore no dead-time-corrected fluxes. Two examples are shown here, both from GOES-13, one from January 2013 (Figure 9) and one from July 2013 (Figure 10).

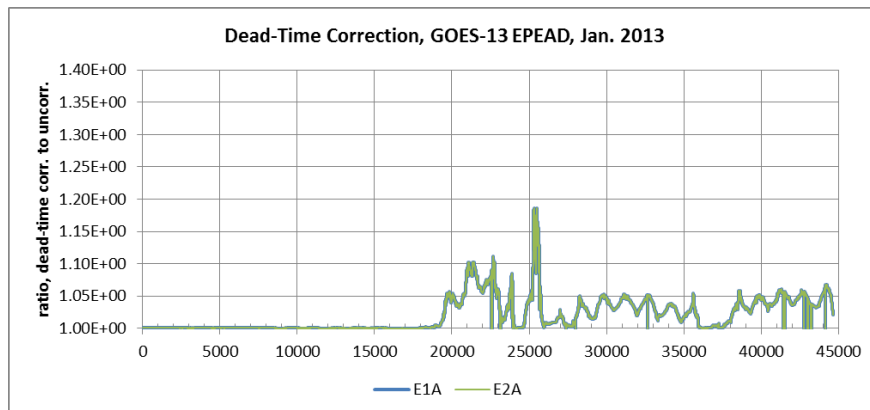


Figure 9. GOES-13, January 2013. Multiplicative dead-time correction for the EPEAD-A sensor.

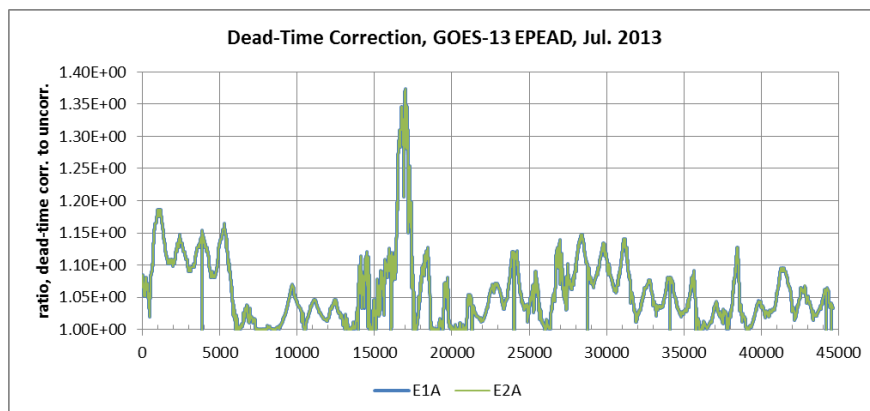


Figure 10. GOES-13, July 2013. Multiplicative dead-time correction for the EPEAD-A sensor.

First, both plots show that the correction is the same for the E1 and E2 channels, as it should be. The curves for the other EPEAD on GOES-13 (not shown) are similar but not identical. At the beginning of January 2013, the dead-time correction was nearly unity, consistent with the low levels shown in Figure 8. On January 13, the correction rises along with the fluxes, and there is a peak in the correction on January 18. The correction was on average higher during July 2013 due to the higher flux levels (Figure 12). It reached a maximum value of 1.37 during several minutes between 1810 and 1910 UT on July 12. (The corresponding correction for EPEAD-B was 1.40.)

To check: the E1 count rate at 1815 UT was 106897.5 c/s and the E2 count rate was 1186.3 c/s. The product of the EPEAD dead time (2.5 microseconds) and the sum of these two rates is 0.2702, and the multiplicative dead-time correction $1/(1-0.2702)$ is 1.37, as expected.

Under the on-orbit compression scheme applied to the EPEAD data, the maximum E1 count rate that is not ‘digitally’ saturated due to the compression scheme is $1949696/4.096\text{s} = 476,000$ c/s, which is much less than the observed count rate in this instance. However, the accuracy of this non-paralyzable dead-time model when the correction is this large is an open issue.

4.3 Error Bars / Sensitivity to Input Errors

The one-sigma error bars (equation 8) are shown in Figure 5, Figure 7, Figure 8, Figure 11 as orange bands around the fluxes. When the fluxes are flagged and replaced with fill values, the associated error bars are as well. Therefore, the largest error bars shown in these plots do not appear in the final product.

4.3 Quality Control Plots

The pitch-angle product algorithm automatically produces a quality control (QC) plot that summarizes the science-quality EPEAD electron fluxes, orientation flag, and data quality flags for a given satellite in a given month. For example, the file name for the GOES-15 QC plot from August 2014 is ‘g15_epead_e13ew_1m_qc_20140801_20140831_science_v1.0.0.pdf.’ Several examples of QC plots are given here.

The top panel shows the orientation flag, along with some words on how to interpret it. The 2nd panel shows the dead-time-corrected E1 and E2 fluxes from EPEAD-A, along with the magnitudes of the E1 and E2 contamination corrections. These corrections are not reported in the final product but are shown here for comparison purposes. The 3rd panel shows the contamination-corrected and flagged fluxes, along with orange bands representing the one-sigma errors. The 4th panel shows the dqfs for E1 and E2. The 5th-7th panels have the same format as the 2nd-4th panels, but show the EPEAD-B quantities. In general, the E1 curves are turquoise (dotted in the case of the dqfs) and the E2 curves are dark blue.

Figure 11 shows a GOES-13 QC plot from March 2012, during which there was a large SEP event. Figure 12 shows a GOES-13 QC plot from July 2013, when elevated electron fluxes as well as dropouts were observed.

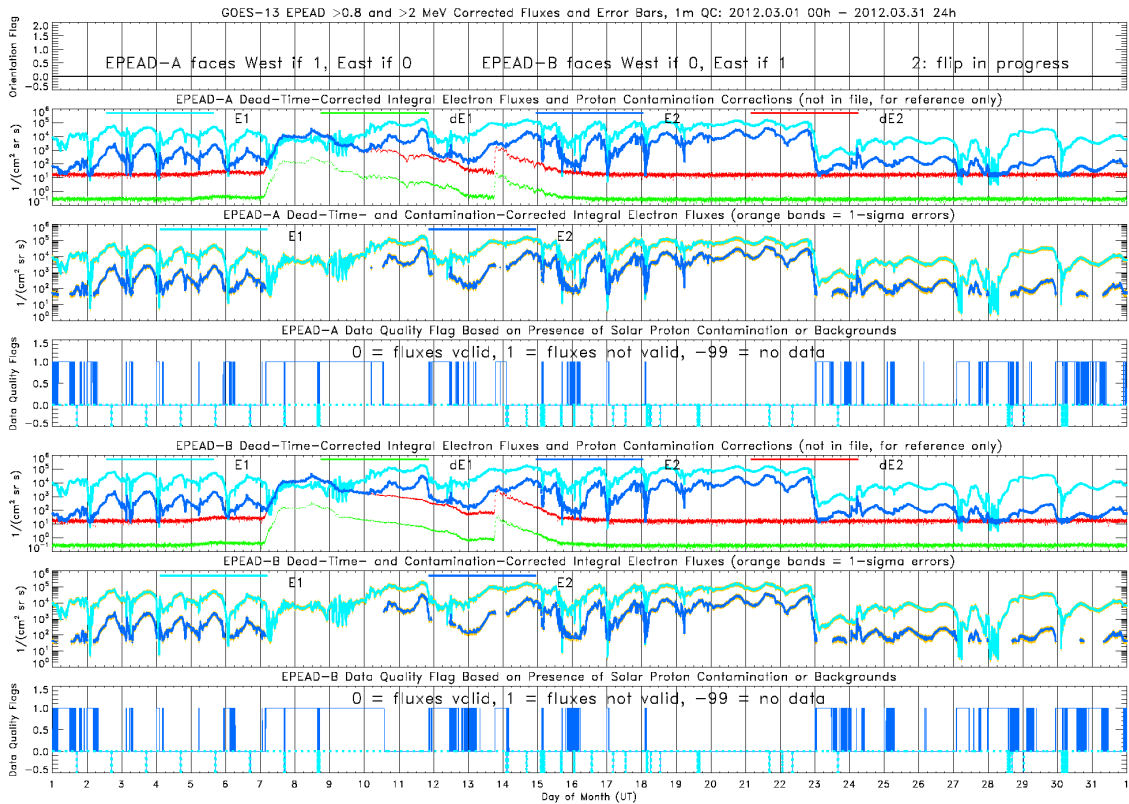


Figure 11. QC plot for GOES-13, March 2012.

GOES EPEAD Science-Quality Electron Fluxes
Algorithm Theoretical Basis Document

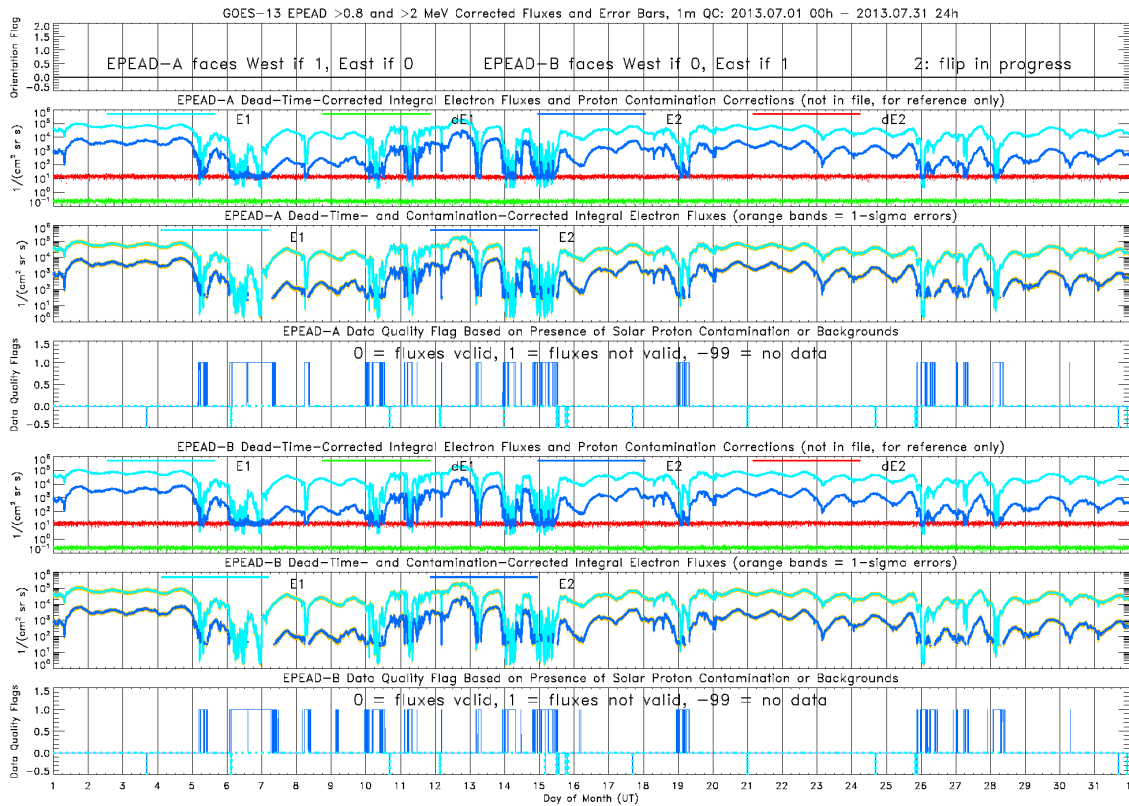


Figure 12. QC plot for GOES-13, July 2013.

5.0 PRACTICAL CONSIDERATIONS

5.1 Numerical Computation Considerations

No special numerical methods are used in implementing this algorithm.

5.2 Programming and Procedural Considerations

Originally developed and tested in IDL 8.2.3 on a 64-bit Windows 7 system. Operating using IDL 8.3 in a Red Hat Enterprise Linux (RHEL) Workstation release 6.5 environment with an Intel Core i7 processor (3325 MHz).

Main script:

```
goesnop_epeade_reprocess_1min
```

Custom procedure/function calls:

```
jvr_days_in_month  
jvr_get_mag_netCDF  
    jvr_unix_epoch_to_jday  
jvr_get_epeade_1min_netCDF  
    jvr_unix_epoch_to_jday  
jvr_get_epeadp_1min_netCDF  
    jvr_unix_epoch_to_jday  
jvr_match_flux_timestamps_funct  
jvr_dead_time_correction_domeD3  
    jvr_set_epead_const  
jvr_contam_corr_epead_ele2  
    jvr_set_epead_const  
jvr_write_epeade_new_ncdf  
    jvr_unix_epoch_to_jday  
    jvr_days_in_month  
    jvr_global_common_epeadnew_1min  
        jvr_jday_to.UTCstr  
jvr_write_epead_orientation_flag_ncdf  
    jvr_unix_epoch_to_jday  
    jvr_days_in_month  
    jvr_global_common_epeadnew_1min  
jvr_plot_goesn_epeade_new_ncdf_auto  
    jvr_unix_epoch_to_jday  
    jvr_xticks_nolabel  
    jvr_xticks_dy
```

5.3 Quality Assessment and Diagnostics

A monthly quality control plot is created showing time series of the orientation flag and the dead-time-corrected fluxes, contamination-corrected fluxes, and data quality flags for each look direction. See section 4.3 for examples.

5.4 Exception Handling

The primary exception handled by the algorithm is fill values in the input data. The NGDC netCDF files use -99999 as a fill value, so these fill values need to be identified and explicitly excluded from calculations.

5.5 Algorithm Validation

See section 4.0.

5.6 Acknowledgments

The development of this product was funded in part by the GOES-R Risk Reduction project and in part by NASA Living with a Star TR&T Interagency Purchase Request #NNH13AV99I to NGDC. Users of these data are encouraged to use the following acknowledgment statement: “The GOES EPEAD electron fluxes, associated quality metrics, and orientation flag were provided by the NOAA National Geophysical Data Center.”

6.0 ASSUMPTIONS AND LIMITATIONS

6.1 Constants to be Re-evaluated

The geometrical factors used in the processing of the EPEAD electrons are approximations whose accuracy depends on the ‘true’ energy spectrum of the measured electrons. For operational processing at SWPC (and in the NGDC reprocessing), a single geometrical factor is applied to the count rates for each channel regardless of the shape of the electron spectrum. Based in part on recharacterizations of the EPEAD performed for GOES 13, 14 and 15, the instrument contractor [GOESN-ENG-048D] recommended effective single geometrical factors and energy thresholds for the three electron channels. (The old geometrical factors were derived by SWPC.) Starting with GOES 13, SWPC is using these new geometrical factors for processing two of the three Energetic Proton, Electron and Alpha Detectors (EPEAD) electron channels (E1 and E3) and a new energy threshold for one of the electron channels (E1). These changes represent reevaluations of the instrument performance, not design changes. The processing of the most heavily used channel (E2) remains unchanged. (For E2, the recommended geometrical factor was only 10% lower than the old factor; therefore, for consistency, the old factor has been kept in use for GOES 13-15.) The changes are summarized in Table 7.

Table 7. Geometrical factors and energies used by SWPC in the real-time processing of EPS/EPEAD electron fluxes.

Channel	GOES 8-12 EPS		GOES 13-15 EPEAD		
	Energy (MeV)	Geometrical Factor (cm ² sr)	Energy (MeV)	Geometrical Factor (cm ² sr)	Increase in Geometrical Factor
E1	>0.6	0.078	>0.8	0.75	9.6x
E2	>2.0	0.05	>2.0	0.05	1.0x
E3	>4.0	0.0175	>4.0	0.056	3.2x

The new factors result in lower fluxes for E1 and E3 compared to the real-time GOES 8-12 processing. The difference between the old and new energy thresholds for E1 reflects the gradual “turn-on” in energy of the channel response to electrons. In the future, the effective geometrical factors and energies should be reevaluated using the bowtie method, which will provide an uncertainty due to natural spectral variability.

These factors do not account for differences in response between flight models, both on the same satellite and on different satellites. *Onsager et al.* [2004] determined that the GOES-8 and GOES-9 EPS >2 MeV electron fluxes agreed well when measurements were made within one hour of local time (and one time series was delayed with respect to the other by their local time separation). Such intercomparisons have not been repeated for other near-conjunctions.

6.2 Input and Output File Contents and Formats

Input Files

Example names for GOES-15, August 2014:

'g15_magneto_1m_20140801_20140831.nc'

'g15_epead_e13ew_1m_20140801_20140831.nc'

'g15_epead_p17ew_1m_20140801_20140831.nc'

Variables used: see Table 1

Output files

Example names for GOES-15, August 2014:

'g15_epead_e13ew_1m_20140801_20140831_science_v1.0.0.nc'

'g15_epead_e13ew_1m_20140801_20140831_science_v1.0.0.csv'

'g15_epead_orientation_flag_1m_20140801_20140831_v1.0.0.nc'

'g15_epead_orientation_flag_1m_20140801_20140831_v1.0.0.csv'

'g15_epead_e13ew_1m_qc_20140801_20140831_science_v1.0.0.pdf'

Variables output: see Table 6

6.3 Performance

Fractional error bars are included in the data set for the contamination-corrected fluxes. These error bars include the effect of calibration error, electron counting statistics and the statistical error of the contamination correction, which itself accounts for the calibration error and counting statistics in the proton channels.

6.4 Pre-Planned Product Improvements

The most important planned improvement is the inclusion of corrected and flagged E3 channel fluxes. It was not included in this present version of the data set because, unlike with E1 and E2, the current correction is not suitable for a science-quality data set. With more than a solar cycle of data available from this channel since GOES 8 was launched, we have gained a perspective on the E3 data that was not available when the current contamination correction was derived in 1995. The E3 channel is best viewed as both a >4 MeV electron channel and a >40 MeV proton channel. Both populations are usually below the background levels in the channel. When only one or the other is above backgrounds, the channel can be treated as an electron or a proton channel. Occasionally, they are both present, in which case the data cannot be used quantitatively without more advanced analysis. Until this improvement is made, we recommend that interested members of the user community use the *uncorrected* E3 fluxes and contact NGDC for assistance in the correct interpretation of these important data.

If this data set is extended to GOES 8-12 EPS electrons, then the possible values of the orientation flag will have to be extended to include '3' indicating a spacecraft spinning slowly in storage mode (e.g., GOES-11).

7.0 REFERENCES

- Bodeau, M. (2010), High energy electron climatology that supports deep charging risk assessment in GEO, 48th AIAA Aerospace Sciences Meeting, AIAA 2010-1608.
- Fennell, J. F., H. C. Koons, M. W. Chen, and J. B. Blake (2000), Internal charging: a preliminary environmental specification for satellites, *IEEE Trans. Plasma Science*, 28, 2029-2036.
- Gannon, J. L., S. R. Elkington, and T. G. Onsager (2012), Uncovering the nonadiabatic response of geosynchronous electrons to geomagnetic disturbance, *J. Geophys. Res.*, 117, A10215, doi:10.1029/2012JA017543.
- Garrett, H. B., and A. C. Whittlesey (2011), *Guide to Mitigating Spacecraft Charging Effects*, JPL Space Science and Technology Series, 222 pp.
- Kress, B. T., M. K. Hudson, and J. Paral (2014), Rebuilding of the Earth's outer electron belt during 8–10 October 2012, *Geophys. Res. Lett.*, 41, 749–754, doi:10.1002/2013GL058588.
- Matthiä, D., T. Berger, A. I. Mrigakshi, and G. Reitz (2013), A ready-to-use galactic cosmic ray model, *Adv. Space Res.*, 51, 329-338.
- O'Brien, T. P. (2009), SEAES-GEO: A spacecraft environmental anomalies expert system for geosynchronous orbit, *Space Weather*, 7, S09003, doi:10.1029/2009SW000473.
- Onsager, T. G., R. Grubb, J. Kunches, L. Matheson, D. Speich, R. Zwickl, and H. Sauer (1996), Operational uses of the GOES energetic particle detectors, in *GOES-8 and Beyond*, edited by E. R. Washwell, Proc. SPIE Int. Soc. Opt. Eng., 2812, 281–290.
- Onsager, T., A. Chan, Y. Fei, S. Elkington, J. Green, and H. Singer (2004), The radial gradient of relativistic electrons at geosynchronous orbit, *J. Geophys. Res.*, 109, A05221, doi:10.1029/2003JA010368.
- Rodriguez, J. V., T. G. Onsager, and J. E. Mazur (2010), The east-west effect in solar proton flux measurements in geostationary orbit: A new GOES capability, *Geophys. Res. Lett.*, 37, L07109, doi:10.1029/2010GL042531
- Sellers, F. B., and F. A. Hanser (1996), Design and calibration of the GOES-8 particle sensors: The EPS and HEPAD, in *GOES-8 and Beyond*, edited by E. R. Washwell, Proc. SPIE Int. Soc. Opt. Eng., 2812, 353–364.

APPENDIX A: PRODUCT VERSIONS

Version numbers are included in the file name and as a global attribute ‘version’ in the file. The modifier ‘science’ in the name (e.g., ‘g15_epead_e13ew_1m_20140801_20140831_science_v1.0.0.nc’) is used to distinguish these files from the files that contain the output of the SWPC real-time processing. It is not used in file names that have no counterpart in SWPC’s output. An example of a v1.0.0 EPEAD electron netCDF file name is ‘g15_epead_e13ew_1m_20140801_20140831_science_v1.0.0.nc’. An example of the associated orientation flag netCDF file name is ‘g15_epead_orientation_flag_1m_20140801_20140831_v1.0.0.nc’.

Version numbers follow the three-number format (x.y.z) used by some space physics data sets in the NASA Goddard Space Physics Data Facility. We use the three numbers to indicate changes as follows:

- x A major change, such as a quantitative correction to the processing algorithm, or a largely new algorithm, that significantly affects the variable values. After such a change, it will be recommended that users replace all downloaded files with the new version. Earlier data will be retrospectively processed to include these changes and files will be replaced on the server.
- y A minor change, such as (for example) the addition of new variables such as error bars. Some users may choose not to replace all downloaded files with the new version, or at least do not need to redo earlier analyses. Earlier data will be retrospectively processed to include these changes and files will be replaced on the server.
- z A patch, such as a correction to metadata. Earlier data will not be retrospectively processed to make this fix until x or y is incremented

The corresponding ATBD version should be x.y.

Version 1.0.0

language = IDL; integral electron flux corrected and flagged using complete set of Sauer coefficients and flagged when data are bad due to solar proton contamination; channel E3 not included in this version.

APPENDIX B: LIST OF VARIABLES AND METADATA

Global attributes:

GOES_satellite: 15
 version: 1.0.0
 version_description: language = IDL; integral electron flux corrected and flagged using complete set of Sauer coefficients and flagged when data are bad due to solar proton contamination; channel E3 not included in this version.
 conventions: GOES Space Weather
 title: GOES Energetic Proton Electron and Alpha Detector Reprocessed Electron Fluxes
 institution: NOAA
 source: Satellite in situ Observations
 satellite_id: GOES-15
 instrument: EPEAD
 process_type: 1-minute Averages
 process_level: Level 2
 sample_time: 1
 sample_unit: minutes
 creation_date: 2014-08-01 20:34:53.000 UTC
 start_date: 2014-03-01 00:00:00.000 UTC
 end_date: 2014-03-31 23:59:00.000 UTC
 records_maximum: 44640
 records_present: 44640
 records_missing: 0
 originating_agency: DOC/NOAA/NESDIS/NGDC
 archiving_agency: DOC/NOAA/NESDIS/NGDC

18 variables in file

```
-----
    0  time_tag  DOUBLE
dims =      0
long_name
Date and time for each observation (beginning of the minute over which the data are
averaged)
units  milliseconds since 1970-01-01 00:00:00.0 UTC
calendar  Gregorian
-----
    1  E1W_DTC_FLUX  DOUBLE
dims =      0
description
```

Average flux of electrons with energy $>.8$ MeV from the A detector that faces East or West depending on the orientation flag (0 = east 1 = west 2 = yaw-flip in progress) corrected for dead time

long_label electrons-1-A ($>.8$ MeV) dtc flux

short_label e1A dtc

plot_label e1A($>.8$ MeV)dtc

lin_log log

units $e/(cm^2 s sr)$

format e12.4

nominal_min 10

nominal_max 1000000

missing_value -99999

2 E1E_DTC_FLUX DOUBLE

dims = 0

description

Average flux of electrons with energy $>.8$ MeV from the B detector that faces East or West depending on the orientation flag (1 = east 0 = west 2 = yaw-flip in progress) corrected for dead time

long_label electrons-1-B ($>.8$ MeV) dtc flux

short_label e1B dtc

plot_label e1B($>.8$ MeV)dtc

lin_log log

units $e/(cm^2 s sr)$

format e12.4

nominal_min 10

nominal_max 1000000

missing_value -99999

3 E2W_DTC_FLUX DOUBLE

dims = 0

description

Average flux of electrons with energy >2 MeV from the A detector that faces East or West depending on the orientation flag (0 = east 1 = west 2 = yaw-flip in progress) corrected for dead time

long_label electrons-2-A (>2 MeV) dtc flux

short_label e2A dtc

plot_label e2A($>.8$ MeV)dtc

lin_log log

units $e/(cm^2 s sr)$

format e12.4

nominal_min 10

nominal_max 1000000

missing_value -99999

4 E2E_DTC_FLUX DOUBLE

dims = 0

description

Average flux of electrons with energy >2 MeV from the B detector that faces East or West depending on the orientation flag (1 = east 0 = west 2 = yaw-flip in progress) corrected for dead time

long_label electrons-2-B (>2 MeV) dtc flux

short_label e2B dtc

plot_label e2B(>2 MeV)dtc

lin_log log

units e/(cm² s sr)

format e12.4

nominal_min 10

nominal_max 1000000

missing_value -99999

5 E1W_COR_FLUX DOUBLE

dims = 0

description

Average flux of electrons with energy >.8 MeV from the A detector that faces East or West depending on the orientation flag (0 = east 1 = west 2 = yaw-flip in progress) with backgrounds removed and proton contamination and dead-time corrected (or fluxes replaced with fill values if contamination is too severe)

long_label electrons-1-A (>.8 MeV) cor flux

short_label e1A fxc

plot_label e1A(>.8 MeV)

lin_log log

units e/(cm² s sr)

format e12.4

nominal_min 10

nominal_max 1000000

missing_value -99999

6 E1E_COR_FLUX DOUBLE

dims = 0

description

Average flux of electrons with energy >.8 MeV from the B detector that faces East or West depending on the orientation flag (0 = west 1 = east 2 = yaw-flip in progress) with backgrounds removed and proton contamination and dead-time corrected (or fluxes replaced with fill values if contamination is too severe)

long_label electrons-1-B (>.8 MeV) cor flux

```
short_label  e1B fxc
plot_label   e1B(>.8 MeV)
lin_log      log
units        e/(cm^2 s sr)
format       e12.4
nominal_min  10
nominal_max  1000000
missing_value -99999
```

```
-----
      7  E2W_COR_FLUX  DOUBLE
dims =      0
```

description

Average flux of electrons with energy >2 MeV from the A detector that faces East or West depending on the orientation flag (0 = east 1 = west 2 = yaw-flip in progress) with backgrounds removed and proton contamination and dead-time corrected (or fluxes replaced with fill values if contamination is too severe)

```
long_label   electrons-2-A (>2 MeV) cor flux
short_label  e2A fxc
plot_label   e2A(>.8 MeV)
lin_log      log
units        e/(cm^2 s sr)
format       e12.4
nominal_min  10
nominal_max  1000000
missing_value -99999
```

```
-----
      8  E2E_COR_FLUX  DOUBLE
dims =      0
```

description

Average flux of electrons with energy >2 MeV from the B detector that faces East or West depending on the orientation flag (0 = west 1 = east 2 = yaw-flip in progress) with backgrounds removed and proton contamination and dead-time corrected (or fluxes replaced with fill values if contamination is too severe)

```
long_label   electrons-2-B (>2 MeV) cor flux
short_label  e2B fxc
plot_label   e2B(>2 MeV)
lin_log      log
units        e/(cm^2 s sr)
format       e12.4
nominal_min  10
nominal_max  1000000
missing_value -99999
```

```
    9  E1W_COR_ERR  DOUBLE
dims =      0
description
Standard deviation (fractional) of average flux of electrons with energy >.8 MeV from
the A detector that faces East or West depending on the orientation flag (0 = east 1 = west
2 = yaw-flip in progress) with backgrounds removed and proton contamination corrected
(replaced with fill values if contamination is too severe)
long_label  electrons-1-A (>.8 MeV) cor flux err
short_label  e1A fxc err
plot_label  e1A(>.8 MeV) err
lin_log     log
units      fractional
format     e12.4
nominal_min  10
nominal_max  1000000
missing_value -99999
```

```
   10 E1E_COR_ERR  DOUBLE
dims =      0
description
Standard deviation (fractional) of average flux of electrons with energy >.8 MeV from
the B detector that faces East or West depending on the orientation flag (0 = west 1 = east
2 = yaw-flip in progress) with backgrounds removed and proton contamination corrected
(replaced with fill values if contamination is too severe)
long_label  electrons-1-B (>.8 MeV) cor flux err
short_label  e1B fxc err
plot_label  e1B(>.8 MeV) err
lin_log     log
units      fractional
format     e12.4
nominal_min  10
nominal_max  1000000
missing_value -99999
```

```
   11 E2W_COR_ERR  DOUBLE
dims =      0
description
Standard deviation (fractional) of average flux of electrons with energy >2 MeV from the
A detector that faces East or West depending on the orientation flag (0 = east 1 = west 2
= yaw-flip in progress) with backgrounds removed and proton contamination corrected
(replaced with fill values if contamination is too severe)
long_label  electrons-2-A (>2 MeV) cor flux err
short_label  e2A fxc err
```

```

plot_label  e2A(>.8 MeV) err
lin_log     log
units      fractional
format     e12.4
nominal_min 10
nominal_max 1000000
missing_value -99999

```

```
-----
12  E2E_COR_ERR  DOUBLE
```

```
dims =      0
```

```
description
```

Standard deviation (fractional) of average flux of electrons with energy >2 MeV from the B detector that faces East or West depending on the orientation flag (0 = west 1 = east 2 = yaw-flip in progress) with backgrounds removed and proton contamination corrected (replaced with fill values if contamination is too severe)

```
long_label  electrons-2-B (>2 MeV) cor flux err
```

```
short_label e2B fxc err
```

```
plot_label  e2B(>2 MeV) err
```

```
lin_log     log
```

```
units      fractional
```

```
format     e12.4
```

```
nominal_min 10
```

```
nominal_max 1000000
```

```
missing_value -99999

```

```
-----
13  E1W_DQF  INT
```

```
dims =      0
```

```
description
```

Data quality flag pertaining to solar proton contamination for fluxes with energy >.8 MeV from the A detector: 0 if contamination is sufficiently small that the correction and electron fluxes are valid 1 if contamination is too large and the electron fluxes are not valid.

```
long_label  EPEAD e1A contam corr dqf
```

```
short_label e1A dqf
```

```
plot_label  e1A contam dqf
```

```
lin_log     lin
```

```
units      flag
```

```
format     i3
```

```
nominal_min 0
```

```
nominal_max 2
```

```
missing_value -99

```

```
-----
14  E1E_DQF  INT
```

dims = 0

description

Data quality flag pertaining to solar proton contamination for fluxes with energy >.8 MeV from the B detector: 0 if contamination is sufficiently small that the correction and electron fluxes are valid 1 if contamination is too large and the electron fluxes are not valid.

long_label EPEAD e1B contam corr dqf

short_label e1B dqf

plot_label e1B contam dqf

lin_log lin

units flag

format i3

nominal_min 0

nominal_max 2

missing_value -99

15 E2W_DQF INT

dims = 0

description

Data quality flag pertaining to solar proton contamination for fluxes with energy >2 MeV from the A detector: 0 if contamination is sufficiently small that the correction and electron fluxes are valid 1 if contamination is too large and the electron fluxes are not valid. (Note: if the flag is set to 1 intermittently throughout an extended period either the contamination correction is borderline too large or the fluxes are close to backgrounds and should be treated with caution.

long_label EPEAD e2A contam corr dqf

short_label e2A dqf

plot_label e2A contam dqf

lin_log lin

units flag

format i3

nominal_min 0

nominal_max 2

missing_value -99

16 E2E_DQF INT

dims = 0

description

Data quality flag pertaining to solar proton contamination for fluxes with energy >2 MeV from the B detector: 0 if contamination is sufficiently small that the correction and electron fluxes are valid 1 if contamination is too large and the electron fluxes are not valid. (Note: if the flag is set to 1 intermittently throughout an extended period either the

contamination correction is borderline too large or the fluxes are close to backgrounds and should be treated with caution.

long_label EPEAD e2B contam corr dqf
short_label e2B dqf
plot_label e2B contam dqf
lin_log lin
units flag
format i3
nominal_min 0
nominal_max 2
missing_value -99

17 ORIENTATION_FLAG INT

dims = 0

description

EPEAD orientation flag. 0: A/W faces East and B/E faces West. 1: A/W faces West and B/E faces East. 2: yaw-flip in progress.

long_label EPEAD orientation flag

short_label orientation

plot_label orientation flag

lin_log lin

units flag

format i3

nominal_min 0

nominal_max 2

missing_value -99